CENTER FOR RADIOPHYSICS AND SPACE RESEARCH
CORNELL UNIVERSITY
ITHACA, NEW YORK

January 1971

NAS9-8018

CRSR 418

PHYSICAL PROPERTIES OF THE APOLLO 12 LUNAR FINES

by

T. Gold, B.T. O'Leary and M. Campbell

to be presented at the Lunar Science Conference in Houston
January 11-14, 1971

PHYSICAL PROPERTIES OF THE APOLLO 12 LUNAR FINES

Apollo 12 Grain Size Analysis

The Apollo 12 lunar fines were subjected to similar grain size analysis to that carried out for the Apollo 11 sample (1). The general appearance and the appearance under the microscope of all samples of fines are rather similar, and the measured optical properties also show small but significant differences only. Although this type of uniformity was expected as a consequence of ground-based optical observations of the moon, it nevertheless has to be emphasized as a remarkable conclusion.

The particle size distribution has been determined by two methods: electron microscopy and sedimentation rate in a column of water. The first was described in the Apollo 11 report and is of greatest value for particle sizes ranging down from 10 microns to less than 0.1 micron; it utilizes scanning electron micrographs of small "sections" of powder. The second method utilizes a sedimentation column which has been improved and perfected more recently.

The water sedimentation column consists of a vertical pipe 70.9 cm long, terminating below in a cubical box of optical glass plate. A photographic flash gun is imaged through a large aperture lens with focus just below the point of entry of the tube. Flash synchronized photographs are taken in a viewing direction perpendicular to the direction of the light. Stray and multiply scattered light is carefully excluded, and as a result the light scattered by a particle as small as 1 micron gives a perfectly recordable image. The water column is heated at the top and the temperature

distribution along it is carefully controlled so that no thermal convection can set in. The particle sizes are deduced by Stokes' Law assuming them to be spherical. While this is of course not accurate, the optical and electron microscope examination showed the particles to be on the whole rather compact shapes, making this error rather small. Freedom from disturbing convection in the column is demonstrated by taking the photographs in pairs with a short duration in between, showing that each group of particles has settled a distance in that short time appropriate to its settling time from the top.

For an absolute measurement this method would perhaps not be sufficiently accurate, both for reasons of the particle shapes and perhaps also their unknown densities. For a comparison the method is very good, and it is much easier to accumulate good statistics than by the method of counting particles under the microscope.

Figure 1 compares the small-size particle size distribution of the Apollo 11 bulk box with that of the Apollo 12 contingency sample; the data, obtained by electron microscopy, are plotted as the cumulative number, per cubic centimeter, of particles larger in size than the abscissa value. A porosity of 0.5 is assumed and the number of particles counted is about 2000 in each case. The two curves are very similar, showing greatest divergence at particle sizes of a few microns; the difference, which amounts to less than a factor 2.5, is probably real. Its significance is shown a little more clearly in Figure 2 in which the differential rather than cumulated particle density is plotted.

The Apollo 12 contingency sample and three core samples have been analyzed by the sedimentation column method, the comparisons are shown on Figures 3 and 4. From these curves it would appear that the surface sample from Apollo 12 is slightly coarser grained than that from Apollo 11. Among the core samples there is also a slight, but nevertheless significant, variation in the grain size distribution, with the deeper samples being richer in small particles than the surface and close subsurface ones. Although the differences between the various samples shown in Figures 3 and 4 are small, the difference between the Apollo 11 and the Apollo 12 surface sample seems to be quite definite, as is the difference of two core samples from the remainder of the Apollo 12 material.

The fact that the grain size distribution in the core sample shows significant differences within tens of centimeters variation of depth requires some comment. If these differences represent layers transported there from different locations, then these layers are evidently only some tens of centimeters in thickness. Since their deposition the ground must not have been mixed up and homogenized on a local scale by small meteorite impacts. The deposition of layers was evidently a faster process than any turning over through the action of meteorites, at any rate at this particular site.

If the soil is generally found to be deposited in layers distinct either in particle size distribution or albedo (as the core photographs clearly suggest) or in chemical composition, (and the Apollo 12 site seems quite representative of most mare ground) then this must have a profound effect on the discussion of the

derivation of the material. Such layers could be derived from the material thrown out in crater-forming events at a distance at which the character of the material was sufficiently different. Layers could be preserved only if the ground was gradually being filled in, faster than it was being plowed over. The probability of adding some tens of centimeters of height per unit time must be greater than the probability of plowing to that depth by a local impact in the same period. The size distribution of meteorites would then have to be very different from the law found at the present time, with a remarkable absence of small meteorites. The law found at the present time would certainly be far on the side of making the ground plowed over locally much faster than filled in from afar. It is for this reason that most investigators believe the moon has been subject to a local "gardening" process.

There is another possibility and it is connected with the hypothesis that the dust is subject to a surface transportation process. If the mare ground is gradually being filled in from material eroded away from higher terrain, then this will produce a layered structure so long as the filling in process is faster than the local meteoritic plowing. Individual layers of ray material from a distant impact would then mostly be preserved by the accumulated overburden. It is then not necessary to invoke a very anomalous size distribution of meteorites in order to preserve layers from distant crater events. In addition the surface transportation process itself may change the source of origin of material reaching a given point, and distinct layers may arise

from this cause also.

Figures 5 and 6 compare the results obtained by electron-microscopy and the sedimentation column method for the Apollo 11 and 12 bulk samples.

Dielectric Constant Measurement

The measurements of the high frequency electrical properties at 450 MHz do not disclose any marked difference in the dielectric constant of powder material from site to site. In Figure 7 the dielectric constant measurements, as a function of bulk powder density, are shown for two Apollo 12 sites--one at a depth of 15 cm below the surface--as well as for the Apollo 11 bulk sample. The two Apollo 12 samples were chosen for their contrasting physical appearances, sample 12033 being much lighter in color and finer in texture than sample 12070. The variation of dielectric constant with density follows the Rayleigh formula (Campbell and Ulrichs, 1969) in all cases and, indeed, a single such curve fits all the data within ±1 percent excepting only the highest density point of sample 12070. The ground-based radar determinations of the dielectric constant are in complete accord with these measurements if one assumes a density of about 1.7 g cm^{-3} for the soil at a depth of 20 cm, an assumption which does no violence to the known properties of the soil.

Also shown on Figure 7 are dielectric constant--density points for four solid lunar rocks, two each from Apollos 11 and 12. The latter pair, 12063 and 12065, are very similar petrologically and lie closely adjacent in the figure. Some allowance should be

made for the porosity (~15%) of sample 10022 but this cannot greatly change the scatter of the points corresponding to this small but not atypical selection of rocks. None of the four solid rocks, nor any mixture of them, could be ground to a powder with the electrical properties of the dust samples, a conclusion in which we concur with the mineralogists.

Figure 8 shows in a similar way the variations with density of the absorption length in the powder samples, with points for the four solid rocks in addition. Again, assuming plausible densities for the powder at depths of a few centimeters, the data agree with prior ground-based radiothermal observations by Troitsky and others.

Optical Properties

The optical reflectivity and polarization of the Apollo 12 soil sample were measured as a function of phase angle with the same instrument and in the same manner as done previously for the Apollo 11 samples (2). Both Apollo 11 and 12 samples were prepared by gradually dropping the fine-grained soil from a height of about 2 cm onto a sample tray.

Figures 9 and 10 indicate the dependence of reflectivity and polarization on phase angle for two viewing angles, ε, of 0° and 60°, as measured from the normal to the surface of the sample. While the Apollo 11 and 12 samples have similar photometric curves, the Apollo 12 sample is noticeably brighter than Apollo 11 (Figure 9). The curves labeled "Moon" are taken from Hapke (3) and normalized to the normal albedo of the Apollo 11 sample. The

Apollo 12 soil has a normal albedo at .56μ wavelength of .125±.003 as compared with .102±.003 for the Apollo 11 sample. Moreover, the Apollo 12 soil is redder than both the Apollo soil and the mean value for the moon (4). Finally, the Apollo 12 soil shows greater reddening with phase angle than the Apollo 11 soil. At $\varepsilon=60^{\circ}$, the photometric functions of both the Apollo 11 and 12 soils indicate a flattening toward larger phase angles compared with the lunar curve. The difference can probably be attributed to large scale roughness of the lunar surface as observed from the earth.

In Figure 10 the polarization of the Apollo 12 soil is very similar to that of the moon as a whole (3). However, for $\varepsilon=60^{\circ}$, both samples show peaks in polarization at greater phase angles than for the moon (5). The maximum polarization from the Apollo 12 sample is in good agreement with earth-based observations, while that of Apollo 11 is anomalously high. The interpretation of these data is somewhat uncertain, however, because of such factors as compaction, interaction with moisture and relative quantities of surface and subsurface soil contained in a given sample.

A study of the dependence of polarization and reflectivity on the degree of compaction, along with spectrophotometry of Apollo 12 soil and rocks, will be reported elsewhere (6).

Figure Captions

Figure 1. The cumulative particle size distribution for the Apollo 11 and 12 bulk fines, determined from electronmicroscope data.

Figure 2. The differential particle size distribution for the Apollo 11 and 12 bulk fines, determined from electronmicroscope data.

Figure 3. The differential particle size distribution for the Apollo 11 and 12 bulk fines, determined with the sedimentation column method.

Figure 4. The differential particle size distribution for the Apollo 12 bulk and core samples, determined with the sedimentation column method.

Figure 5. Differential particle size distribution for the Apollo 11 bulk fines. Curve fits the electron microscope data, sedimentation data are also shown.

Figure 6. Differential particle size distribution for the Apollo 12 bulk fines. Curve fits the electron microscope data, sedimentation data are also shown.

Figure 7. Dielectric constant measurements for two Apollo 12 powder samples and the Apollo 11 bulk sample, as a function of bulk powder density. Dielectric constant vs. density points for four solid lunar rocks are also shown.

Figure 8. The variation with density of the absorption length in two Apollo 12 powder samples and the Apollo 11 bulk sample. Points for four solid rocks are also shown.

Figure 9. (a) Reflectivity of the Apollo 11 and 12 soil vs phase angle at .56μ wavelength for viewing angles $\varepsilon=0^\circ$ and 60°. (b) Color index B-V of the powder samples vs phase angle for $\varepsilon=0^\circ$. Also plotted are (c) the reddening junction of the entire moon, as determined by Gehrels et al. (4), and (d) B-V values for a region of Mare Tranquillitatis.

Figure 10. The polarization of the Apollo 11 and 12 powders vs phase angle at .56μ wavelength for viewing angles $\varepsilon=0^\circ$ and 60°.

References

1. T. Gold, M. J. Campbell and B. T. O'Leary, Science 167, 707 (1970).

2. B. O'Leary and F. Briggs, J. Geophys. Res. 75, 32, 6532 (1970).

3. B. Hapke, Science 159, 76 (1968).

4. T. Gehrels, T. Coffeen, and D. Owings, Astron. J. 69, 826 (1964).

5. S. F. Pellicori, Astron. J. 74, 1066 (1969).

6. F. Briggs and B. O'Leary, in preparation.

7. We wish to thank Dr. Elizabeth Bilson for assistance with the sedimentation column work, Mr. Frank Briggs for assistance with optical studies, and Miss Joan Winters for assistance with electron microscope particle size counts. Mr. H. J. Eckelmann and Mr. S. M. Colbert helped in the design of the sedimentation column.

We wish to acknowledge gratefully the assistance given us by the Instrumental Analysis Research Department of the Corning Glass Works with scanning electron microscope work.

8. Work on lunar samples was carried out under NASA Contract NASA NAS9-8018.

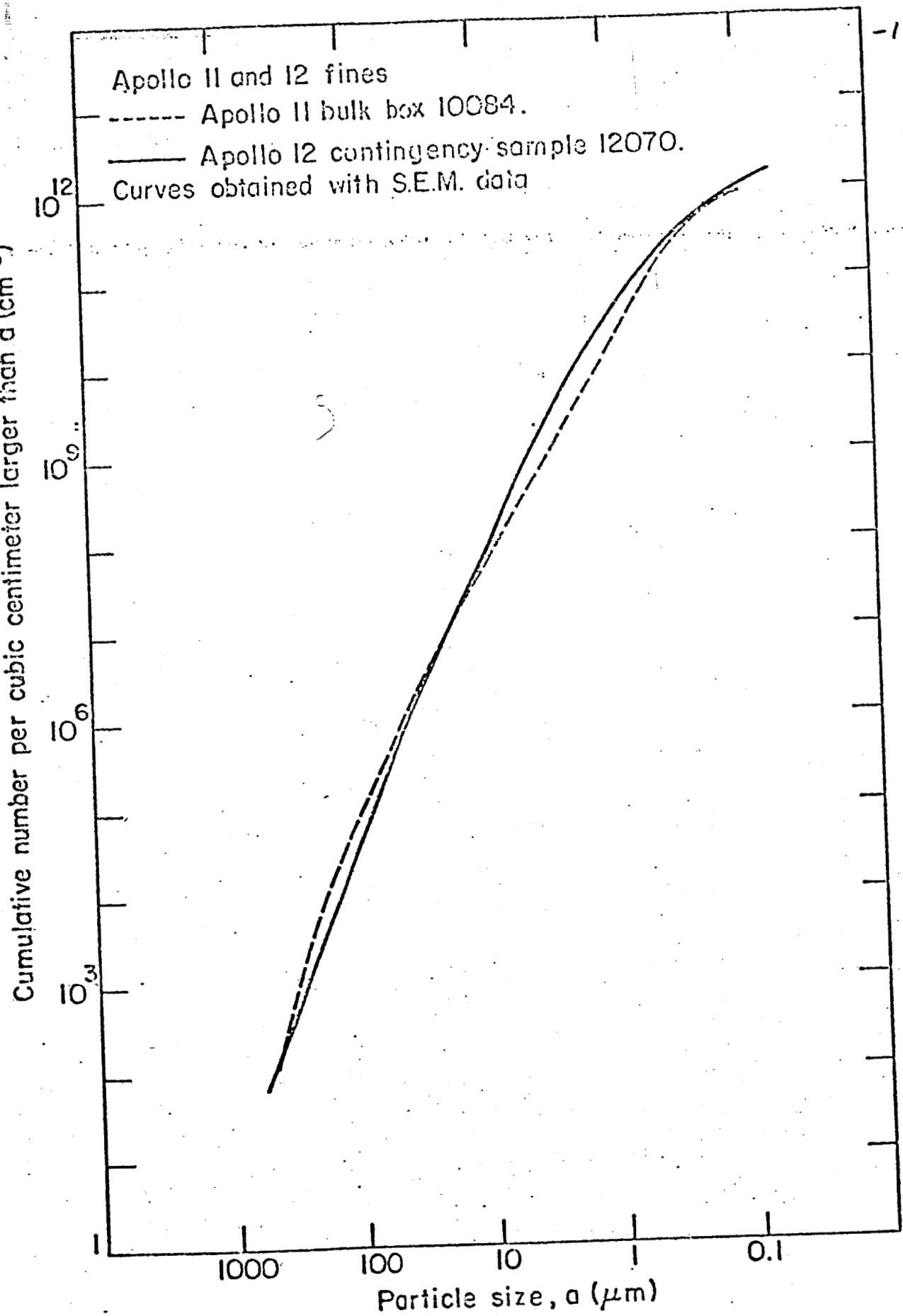
Apollo 11 and 12 fines
------ Apollo 11 bulk box 10084.
—— Apollo 12 contingency sample 12070.
Curves obtained with S.E.M. data
Cumulative number per cubic centimeter larger than a (cm⁻³)
10¹²
10⁹
10⁶
10³
1
1000
100
10
1
0.1
Particle size, a (μm)

FIG. 1

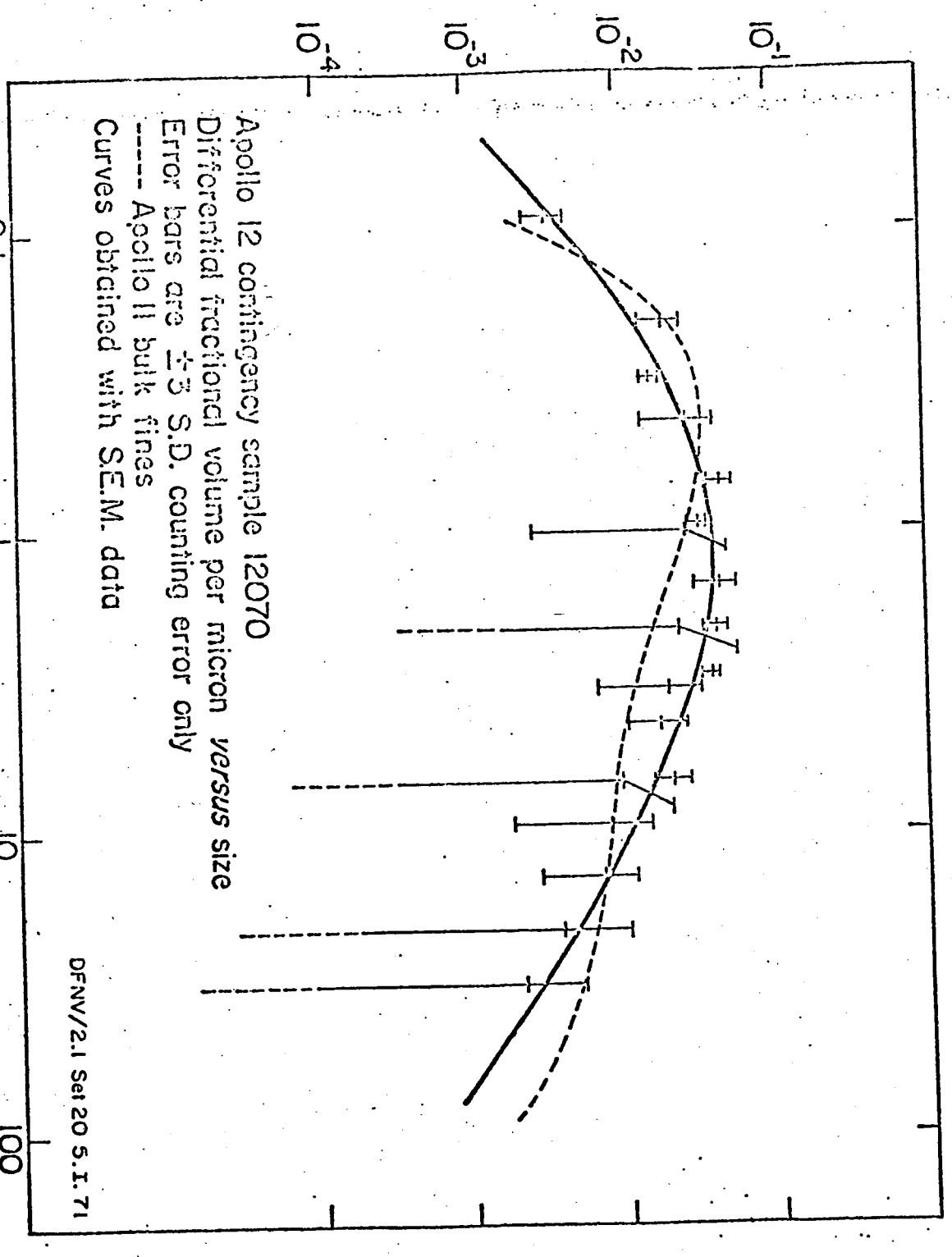
10^{-1}
10^{-2}
10^{-3}
10^{-4}
0.1
1.0
10
100
Particle size, μm
Apollo 12 contingency sample 12070
Differential fractional volume per micron *versus* size
Error bars are ±3 S.D. counting error only
----- Apollo 11 bulk fines
Curves obtained with S.E.M. data
DFNV/2.1 Set 20 5.I.71

Fig. 2

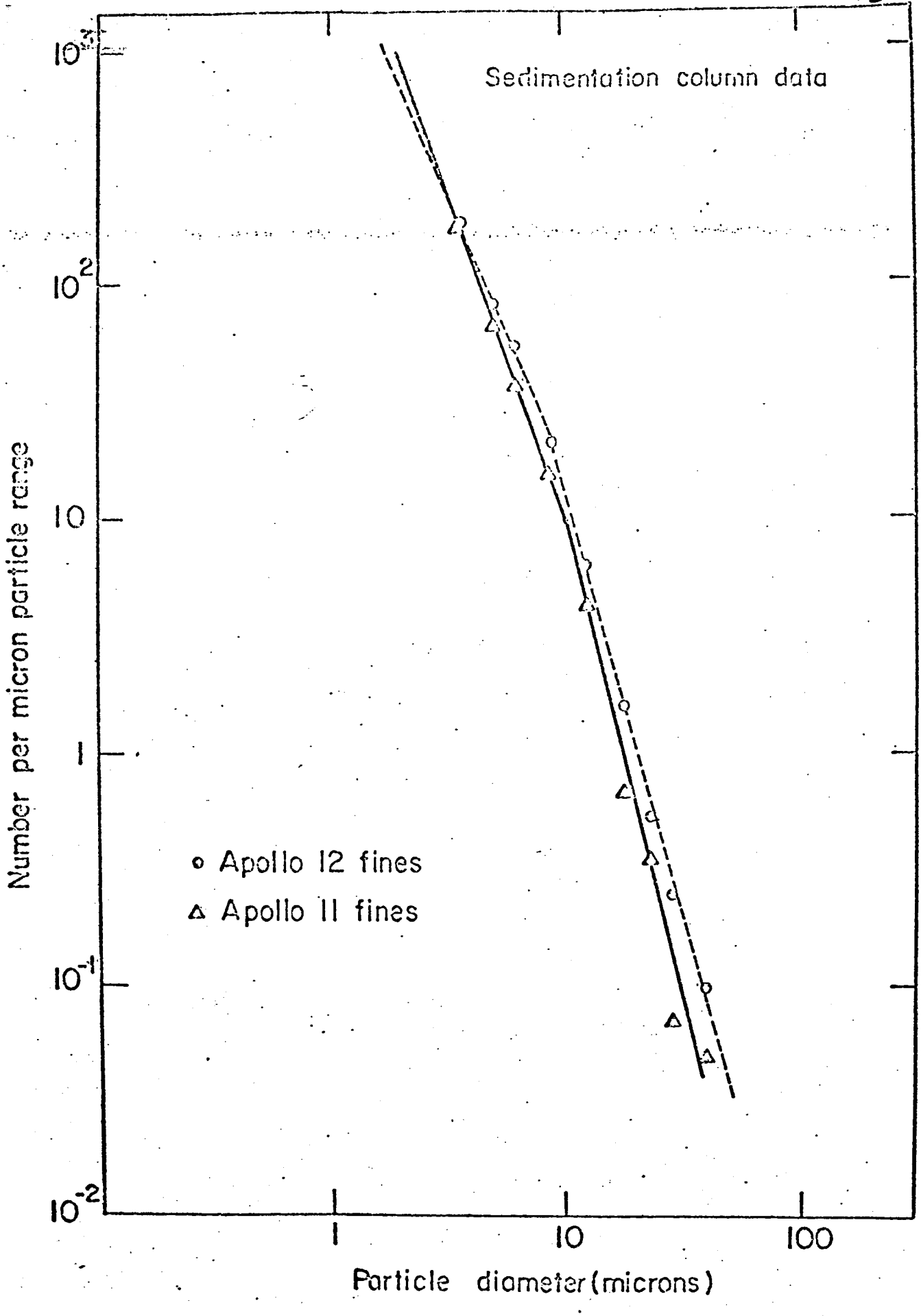
Sedimentation column data
Number per micron particle range
10^{3}
10^{2}
10
1
10^{-1}
10^{-2}
o Apollo 12 fines
Δ Apollo 11 fines
1
10
100
Particle diameter (microns)

FIG. 3

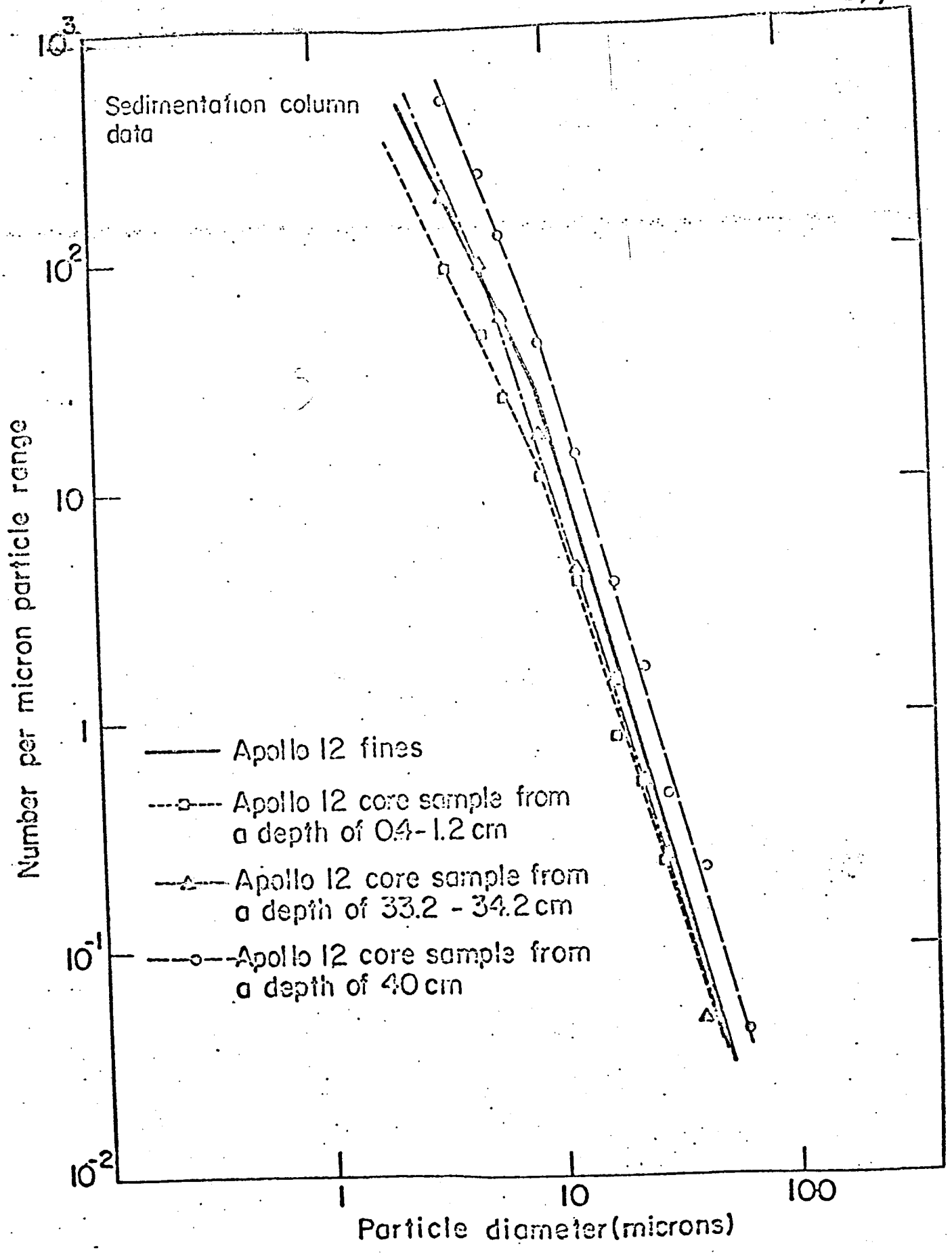
Sedimentation column data
Number per micron particle range
10^3
10^2
10
1
10^{-1}
10^{-2}
1
10
100
Particle diameter (microns)
Apollo 12 fines
Apollo 12 core sample from a depth of 0.4 - 1.2 cm
Apollo 12 core sample from a depth of 33.2 - 34.2 cm
Apollo 12 core sample from a depth of 40 cm

Fig. 4

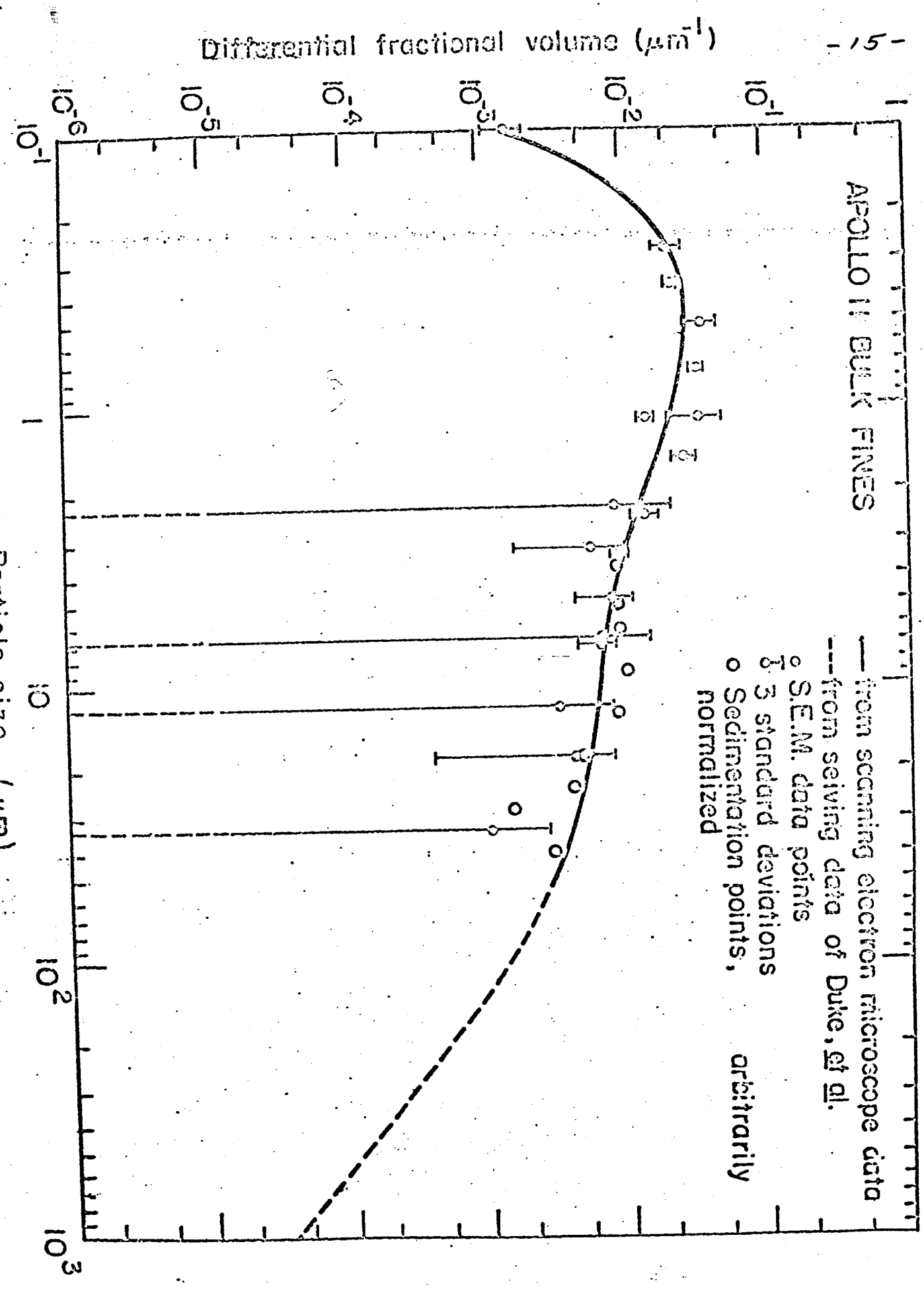
Differential fractional volume (μm^{-1})
10^{-1}
10^{-2}
10^{-3}
10^{-4}
10^{-5}
10^{-6}
1
10
10^2
10^3
Particle size (μm)
APOLLO 11 BULK FINES
— from scanning electron microscope data
--- from sieving data of Duke, et al.
° S.E.M. data points
⊥ 3 standard deviations
o Sedimentation points, normalized
arbitrarily

Fig. 5

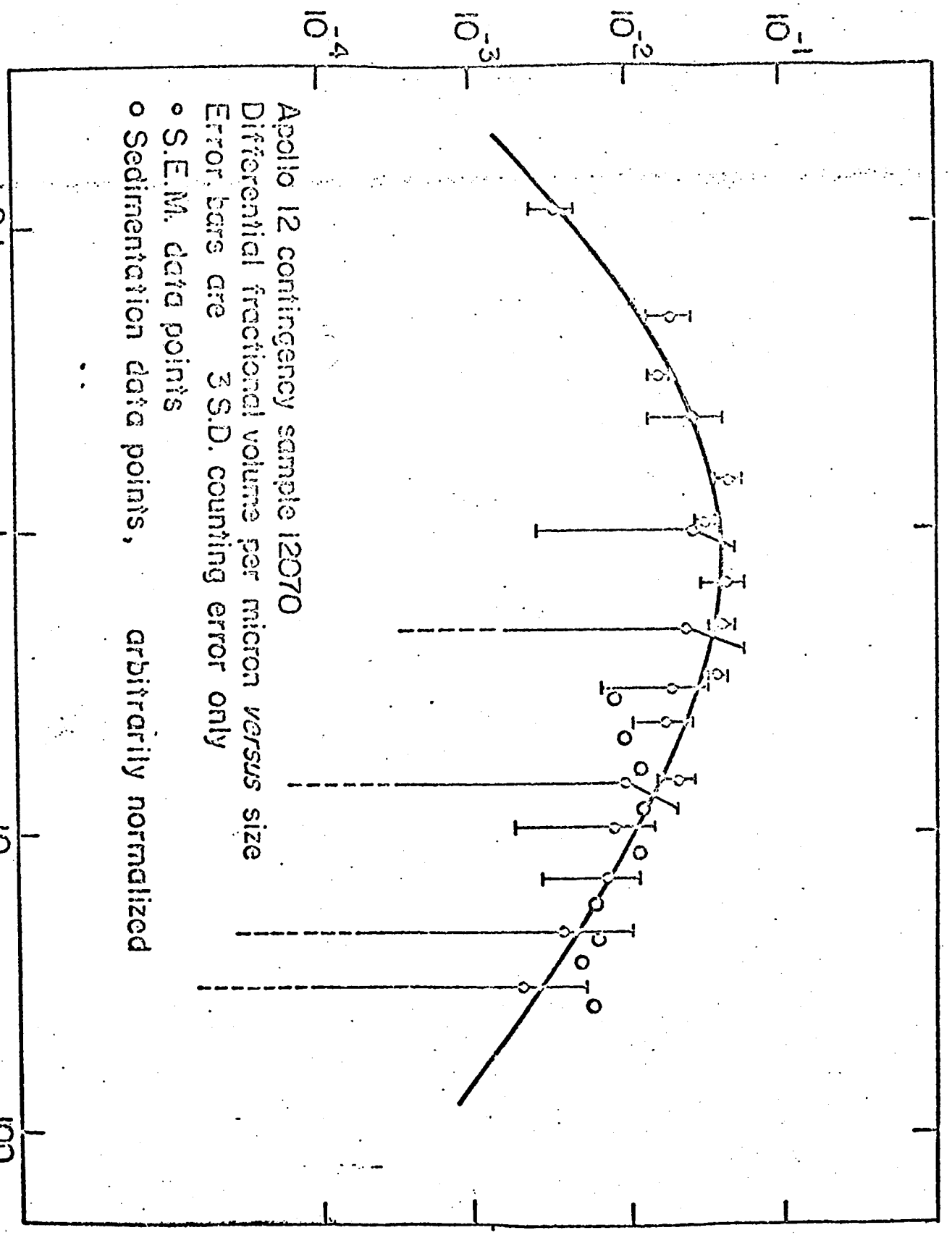
Apollo 12 contingency sample 12070
Differential fractional volume per micron versus size
Error bars are 3 S.D. counting error only
• S.E.M. data points
o Sedimentation data points,
arbitrarily normalized
Particle size, μm
0.1
1
10
100
10-1
10-2
10-3
10-4

Fig. 6

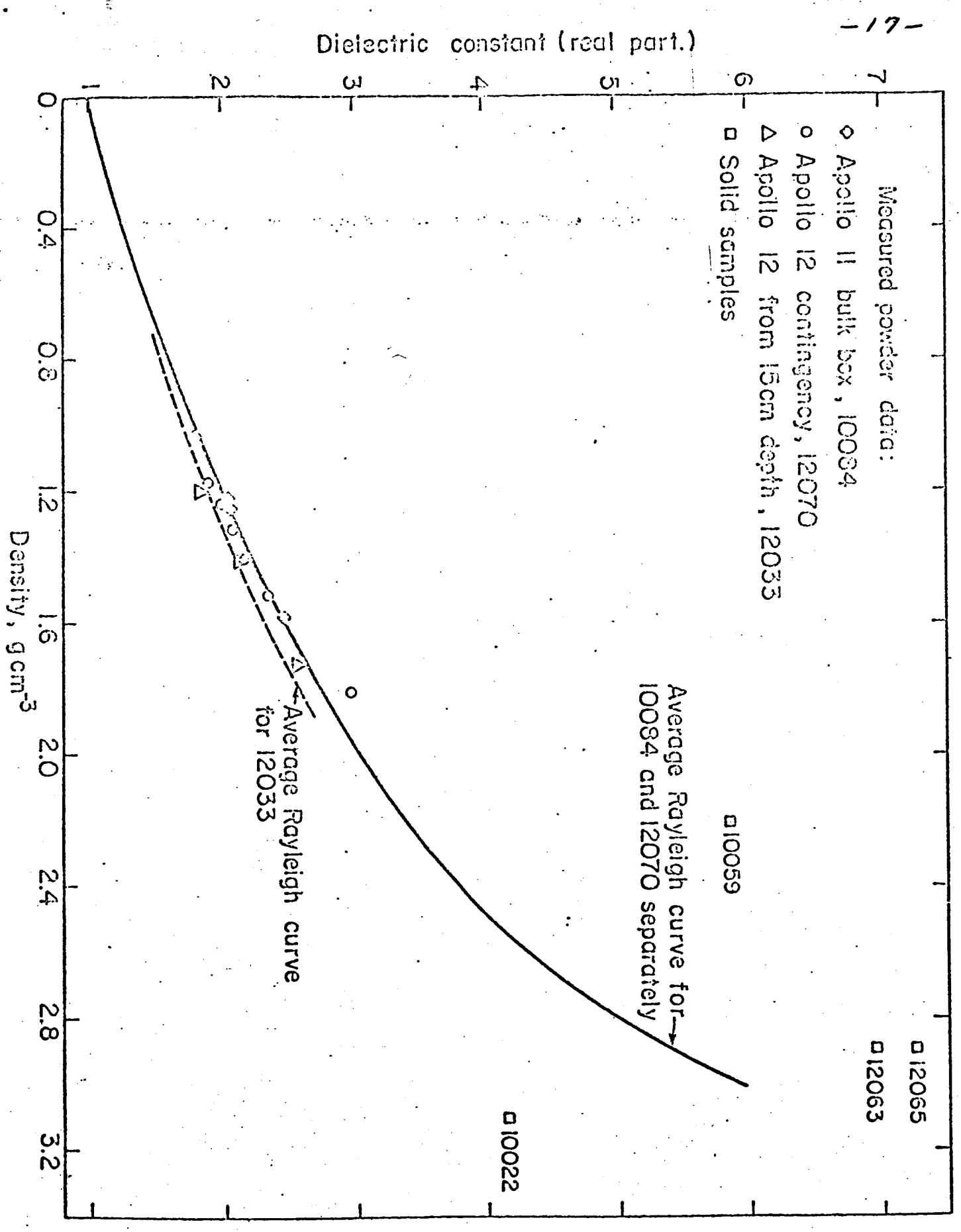
Dielectric constant (real part.)
1
2
3
4
5
6
7
Density, g cm^{-3}
0
0.4
0.8
1.2
1.6
2.0
2.4
2.8
3.2
Measured powder data:
◇ Apollo 11 bulk box, 10084
○ Apollo 12 contingency, 12070
△ Apollo 12 from 15cm depth, 12033
□ Solid samples
□ 12065
□ 12063
□ 10059
□ 10022
Average Rayleigh curve for 10084 and 12070 separately
Average Rayleigh curve for 12033

Fig. 7

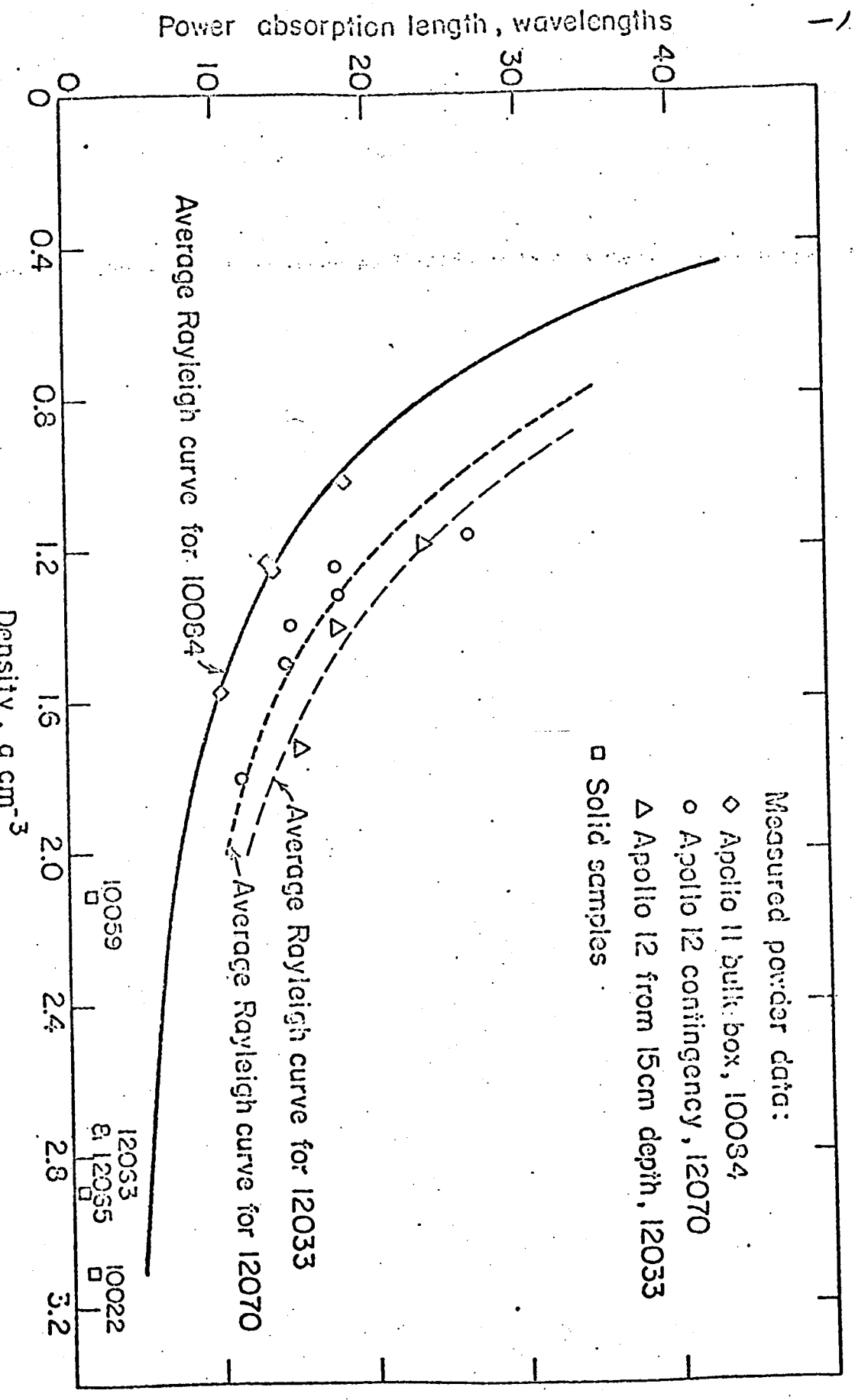
Power absorption length, wavelengths
0
10
20
30
40
0
0.4
0.8
1.2
1.6
2.0
2.4
2.8
3.2
Density, g cm⁻³
Measured powder data:
◇ Apollo 11 bulk box, 10084
○ Apollo 12 contingency, 12070
△ Apollo 12 from 15cm depth, 12033
□ Solid samples
Average Rayleigh curve for 10084
Average Rayleigh curve for 12033
Average Rayleigh curve for 12070
10059
12063
& 12065
10022

Fig. 2

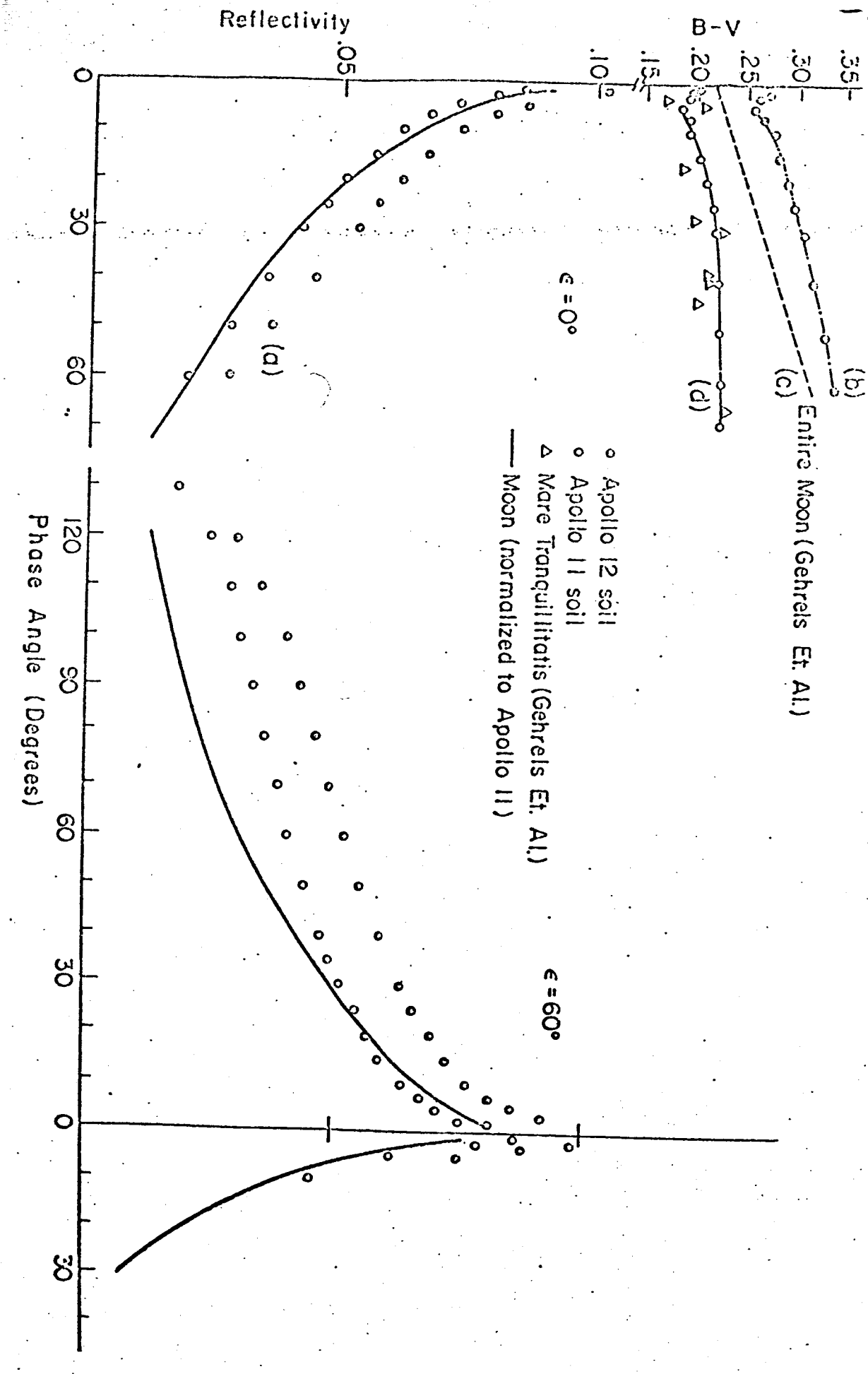
Reflectivity
B-V
.35
.30
.25
.20
.15
.10
.05
0
30
60
(a)
(b)
(c)
(d)
Entire Moon (Gehrels Et. Al.)
ε = 0°
ε = 60°
Apollo 12 soil
Apollo 11 soil
Mare Tranquillitatis (Gehrels Et. Al.)
Moon (normalized to Apollo 11)
120
90
60
30
0
30
Phase Angle (Degrees)

Fig. 9

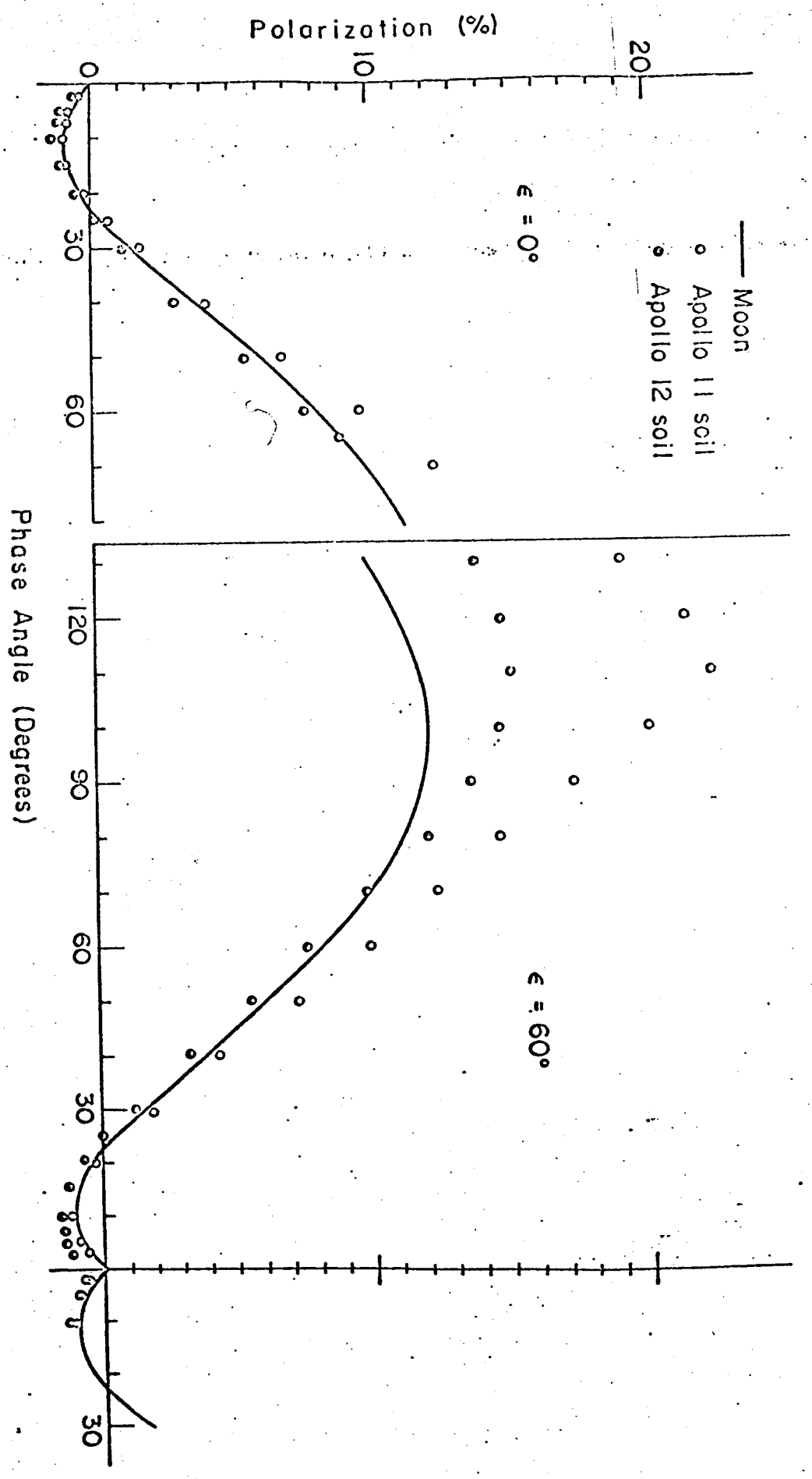
Polarization (%)
0
10
20
30
60
ε = 0°
Moon
Apollo 11 soil
Apollo 12 soil
Phase Angle (Degrees)
120
90
60
30
ε = 60°
30

Fig. 10